Mixed convection drag force on a small particle

Elaad Mograbi,[1] Alexander Vikhansky[2], and Ezra Bar-Ziv[1,2]

[1]Department of Mechanical Engineering
[2]Department of Environmental Engineering
Ben-Gurion University of the Negev
P.O.Box 653, 84105 Beer-Sheva, Israel

Experimental and numerical investigation of the drag force on a small spherical particle in mixed convection is conducted. Data is presented for highly non-isothermal conditions. The ranges of flow regimes are from pure free convection via strong mixed convection patterns to forced convection under non-isothermal conditions. A simple but comprehensive similarity law valid for both co-flow and opposed flow (including reversed flow) is presented.

1. Introduction

A positive temperature difference between a small particle and an infinite quiescent medium will engage buoyancy driven flow opposed to gravity (free convetion). External uniform flow is imposed far from the particle (forced convection). In this problem mixed convection flow patterns prevails. Two cases are considered: (i) the external velocity is opposite to gravity hence it assists the free convection, this case is designated co-flow (or assisting flow); (ii) the direction of the external velocity coincides with gravity hence it opposes the free convection flow, it is designated opposed flow.

Early theoretical results related to mixed convection phenomena are available. Zel'dovich [1] (for details see Ref. [2]) investigated the similarity in a freely rising laminar convective wake far above a hot body. Gutman [3] and Fujii [4] studied the laminar convection above a point heat source. Hieber and Gebhart [5] considered asymptotic expansion for small mixed convection parameter $\xi=Gr/Re^2$. Acrivos and Taylor [6], Brenner [7], Dennis et al. [8] investigated the heat and mass transfer for small Peclet numbers in forced convection dominated regime. These results assume ad hoc the solution to the velocity field, thus offer no new insight to the behavior of the drag. Other related studies are those of Chen and Mucoglu [9, 10], Wong et al. [11] and Cameron et al. [12]; these works are primarily concerned with mathematical solution to the reduced boundary layer equations. This is plausible only when the characteristic width of the boundary layer is small compared to the characteristic length of the particle, i.e. either for large Reynolds number or small buoyancy. Hence, the techniques developed and the results obtained therein cannot be applied for the small particle problem. A Recent experimental study has been performed on the mixed free-forced convection phenomenon on small particles [13-16].

As can be deduced from the above arguments the problem of the drag on a small spherical particle due to the action of strong mixed convection flow field is far from being solved. In this work we present a scaled analysis equation supported by numerical and experimental results which will confirm the existence of a simple similarity law that constitute a natural generalization of the results obtained by

Zel'dovich [1,2]. This result will hold as will be proved for the co-flow and the opposed flow regimes.

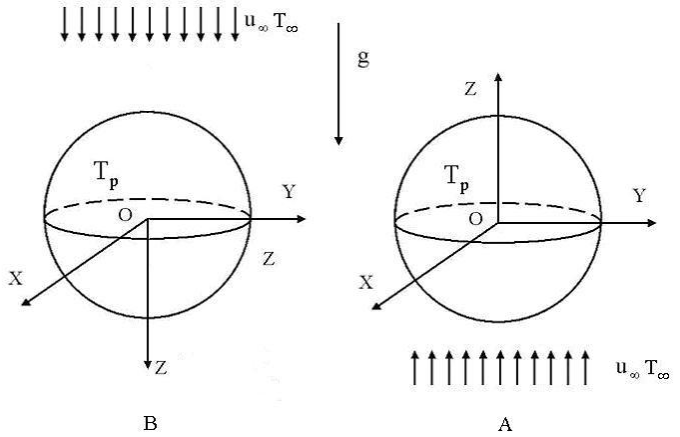

Fig. 1: Schematic view of the problem and coordinates: (A) co-flow regime; (B) opposed flow regime

2. Analysis

2.1 Numerical model

A steady state solution for the transport equations mass, momentum and energy is considered for a stationary sphere with uniform temperature as shown in Fig. 1. We consider high particle-fluid temperature differences, thus the fluid properties are known functions of temperature. The equations are

$$\nabla \cdot (\rho \mathbf{u}) = 0\,, \tag{1}$$

$$\rho(\mathbf{u} \cdot \nabla)\mathbf{u} = -\nabla p + \nabla\{\mu[\nabla \mathbf{u} + (\nabla \mathbf{u})^{T}]\} + \rho \mathbf{g}\,, \tag{2}$$

$$\rho c_p (\mathbf{u} \cdot \nabla)T = \nabla(k \nabla T)\,, \tag{3}$$

where **g** is the gravity acceleration vector, ρ, **u**=(u_x,u_y,u_z), p, T, ν, μ=ρν, c_p and k are density, velocity, pressure, temperature, kinematic viscosity, dynamic viscosity, specific heat and thermal conductivity of the fluid, respectively.

The boundary conditions are

$$\mathbf{u}=0,\ T=T_p \text{ for } |r|=d/2, \tag{4}$$

$$u_x \to 0,\ u_y \to 0,\ T \to T_\infty \text{ for } |r| \to \infty, \tag{5}$$

$$u_z \to u_\infty \text{ for } z \to -\infty. \tag{6}$$

Zel'dovich [1,2] showed that the velocity of the convective wake far upstream from the particle is constant, thus the boundary condition is

$$\frac{\partial u_z}{\partial z} \to 0 \text{ for } z \to \infty. \tag{7}$$

In the opposed flow regime where free convection is dominant the above assumption cannot be applied due to the buoyancy driven flow which is opposite to the external stream, thus, the boundary condition, Eq. (7) must be modified. This problem prompts a large computational domain of about 2000d on the boundary of which it is assumed that pressure is uniform, i.e.

$$p \to p_\infty \text{ for } z \to \infty. \quad (8)$$

The numerical scheme was shown to converge using this boundary condition.

2.2 Scale analysis

For the sake of argument we First consider Boussinesq approximation of the above equations (later we will correct this approximation). Temperature variations are taken into account only in the third term of Eq. (2), $\Delta\rho/\rho=-\beta t$ where β is coefficient of thermal expansion, ρ is some reference density and t is temperature variation. Next we normalize Eqs. (1)-(3) by use of $U=\nu/d$ and d as characteristic velocity and length, respectively. Introducing dimensionless (primed) variables via the relations, $\mathbf{u}=U\mathbf{u}'$, $\mathbf{r}=d\mathbf{r}'$, $p=\rho U^2 p'$ and $T=tT'$; Eqs. (1)-(3) read:

$$\nabla' \cdot \mathbf{u}' = 0, \quad (1')$$

$$(\mathbf{u}' \cdot \nabla')\mathbf{u}' = -\nabla' p' + \nabla'^2 \mathbf{u}' - \mathrm{Gr} T' \mathbf{z}, \quad (2')$$

$$(\mathbf{u}' \cdot \nabla')T' = 1/\mathrm{Pr}\, \nabla'^2 T', \quad (3')$$

where $\mathrm{Gr}=g\beta t d^3/\nu^2$ is the Grashof number, $\mathrm{Pr}=\mu c_p/k$ is Prandtl number and $\mathbf{z}$ is upward directed unit vector. $\mathrm{Re}=u_\infty d/\nu$ enters the above problem through the boundary condition (6):

$$u'_z \to \mathrm{Re} \text{ for } z' \to -\infty. \quad (6')$$

Eqs. (2') and (6') implies that for low Re and Gr the velocity near the particle is due to the external flow, u_∞, and the thermal convective velocity U_{fc}, which will be specified below. Thus, the expression for the drag reads:

$$F_D \sim \rho\nu d u = \rho\nu d(u_\infty + U_{fc}) = \rho\nu^2 \mathrm{Re} + \rho\nu d U_{fc}. \quad (9)$$

The first term in the above equation is the Stokes drag force, while the second is the force that is induced by free convection. As mentioned above, U_{fc} has no exact solution. One can estimate U_{fc} by comparing the convective and the buoyancy terms in Eq. (2'), this gives the relation $(u')^2 \sim \mathrm{Gr}$. Far above the sphere the dominant convective term is the longitudinal component, thus we may substitute for the scaled velocity the expression $u'=U_{fc}d/\nu$ and we conclude that $U_{fc} \sim \nu/d\sqrt{\mathrm{Gr}}$. This is an implicit consequence of the result obtained by Ze'ldovich [1, 2]. Eq. (9) can now be rewritten as:

$$F_D \sim \rho\nu^2(\mathrm{Re}+\mathrm{Gr}^{1/2}). \quad (10)$$

Equation (10) was derived under the assumptions that the temperature dependence of viscosity can be neglected, and that there is no interaction between forced and free convection.

Considering the second term in Eq. (10); for the highly non-isothermal case the viscosity of the gas changes considerably and consequently increases the drag force, thus Gr is a none-unique dimensionless group that defines the problem. The second parameter is a dimensionless viscosity $\mu'=\mu/\mu_\infty$. On the other hand the convective wake weakens due to the external velocity, Therefore, the second term in Eq. (10) depends on Re as well. Hence

$$F_D = F_f + F_{fc}(\mathrm{Gr}, \mu')\phi(\mathrm{Re}) = F_f(\mathrm{Re}, T_p) + \psi(\mu')\,\mathrm{Gr}^{1/2}\phi(\mathrm{Re}). \quad (11)$$

F_f represent the forced convection contribution taking into account the temperature field and non-linear perturbations, these effects have already been studied [17, 18].

$F_{fc}(Gr,\mu')$ is the pure free convection induced drag force that acts on the particle in the absence of the external flow field. $\phi(Re)$ is a rapidly decreasing function of Re, satisfying $\phi(0)=1$ and $\phi(Re\rightarrow\infty)\sim 0$; this can be readily obtained by considering the limiting cases of Eq. (11): For Re approaching zero F_D must reduce to F_{fc}; alternatively, for large Re, F_{fc} must vanish. $\psi(\mu')$ is a function of the dimensionless viscosity. In the next sections we will validate the functional form obtained by Eq. (11) by full numerical solution of Eqs. (1)-(3) with boundary conditions (4)-(8).

3. Experimental Validation

The main concern in the analyses of hydrodynamics is the validity of numerical simulations, which occasionally is unsatisfactory. Here we will establish the validity of our numerical scheme by comparing the results with experiments conducted in an electrodynamic chamber (EDC) [19].

It must be noted that the problem of flow within the EDC is quite different from that of a particle in an infinite medium. This is due to the complex geometry of the EDC, the different boundary conditions and its finite and quite small dimensions (about 200d). We have established a computational domain similar to the EDC geometry and compared the experimental results with the numerical simulations for 80μm diameter a particle.

Figure 2 presents the results of the opposed flow regime for the drag force induced by mixed convection versus drag force induced by forced convection at isothermal conditions-F_D/mg vs. $F_f(T_\infty)$/mg-for three particle temperatures, 365, 466, 586 ^oK. The outcome as one can see is very convincing.

Figure 3 shows the comparison of the free convection induced drag force as function of temperature for different particle diameters (The experimental results are taken from Katoshevski et al. [13]). Again the results are compatible.

Figure 4 presents two graphs of the co-flow induced drag forces F_D/mg vs. $F_f(T_p)$/mg for the three particle temperatures of Fig. 3, the left and the right plots show the numerical and experimental results, respectively. It is evident that the behavior is almost identical in both cases.

Establishing the validity of the numerical scheme we may now turn to the main problem, a particle in an infinite medium.

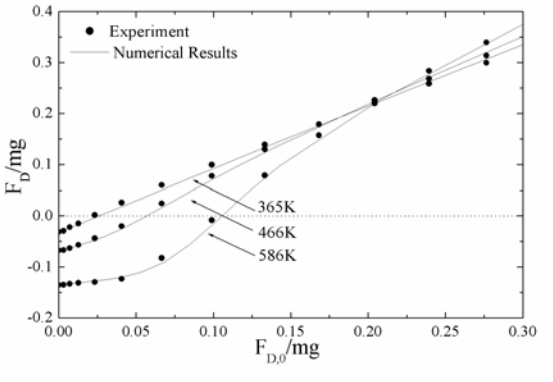

Fig. 2: Comparison of experimental with numerical results of the normalized opposed flow induced drag force F_D/mg versus F_f/mg for particle diameter d_p=80 μm and three surface temperatures, 365, 466, 586 K, with ambient temperature of 298 K.

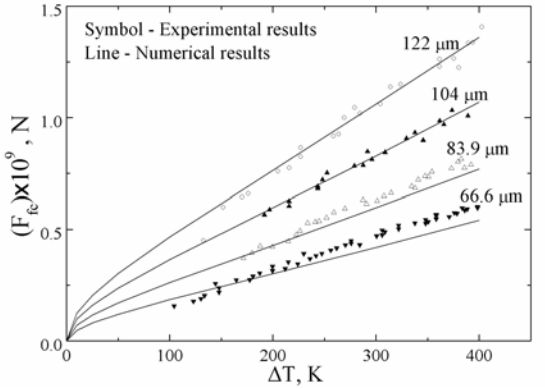

Fig. 3: Comparison of numerical (solid lines) and experimental (scattered points) results for free convection induced drag vs. temperature difference for four particles with diameters of 66.6, 83.9, 104, 122 μm.

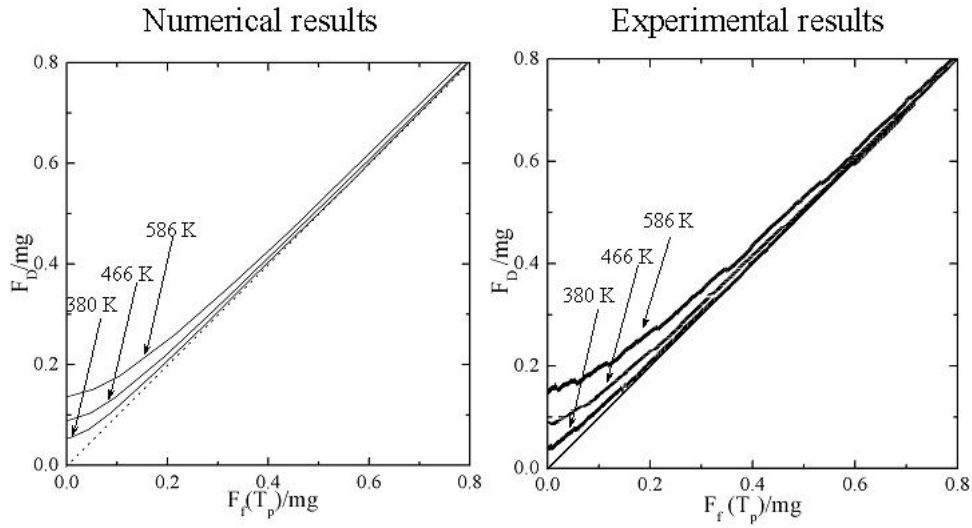

Fig. 4: Comparison of numerical and experimental results for the overall drag force vs. forced convection drag force for the particle of Fig. 2.

4. Discussion

4.1 Free convection

Following the discussion in the analysis leading to Eq. (11), we plot numerical results of $F_{fc}/(\rho v^2 Gr^{1/2})_\infty$ vs. μ', as shown in Fig. 5. The figure illustrates four plots at different diameters collapsing to a straight line. This behavior accounts for the highly non-isothermal condition discussed earlier. We conclude that $F_{fc}(Gr, \mu') \sim \mu' Gr^{1/2}$.

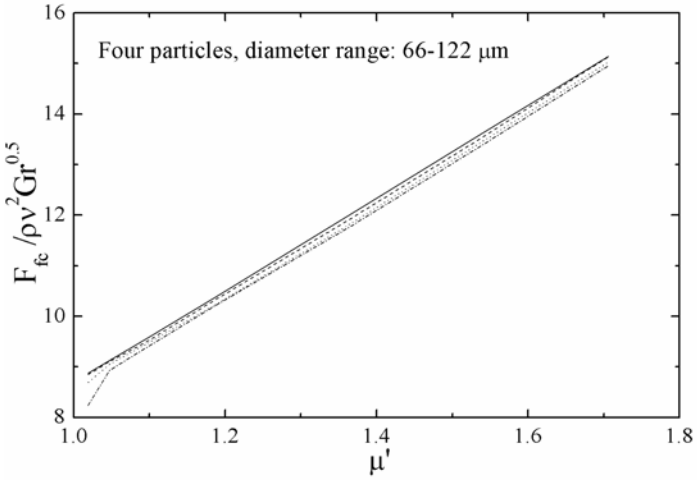

Fig. 5: $F_{fc}/\rho v^2\sqrt{Gr}$ vs. μ' for different particle diameters.

4.2 Co-flow

Figure 6 shows numerical results for the function ϕ vs. Re_f (subscript-f denotes parameters calculated at the film temperature, $T_f=(T_p+T_\infty)/2$). All numerical results fit a similar behavior indicating that the function ϕ depends on Re_f only, as suggested by Eq. (11). Note that matching of the data require the use of the parameter Re_f as opposed to Re, i.e. minor temperature dependence has to be accounted for also in the

function ϕ(Re). We conclude from the results that for the co-flow configuration the argument leading to Eq. (11) was adequate.

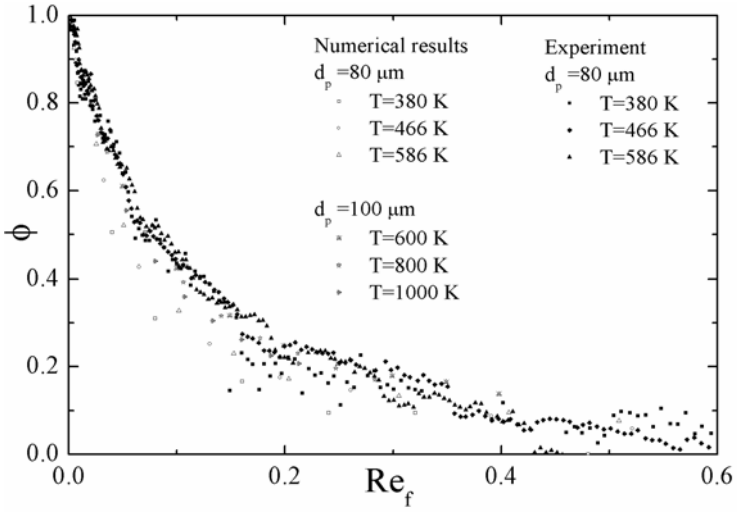

Fig. 6: Experimental and numerical results for the co-flow regime of the function ϕ vs. Re_f. In the figure are presented results for the particle of Fig. 7, as well as a 100 μm particle at 600, 800, 1000 K, with ambient temperature of 298 K.

4.3 Opposed flow

Figure 7 shows the numerical results of the function $\phi(Re_f)$ versus Re_f for the opposed flow for temperatures 466, 586, 1000 ^oK and particle diameter, d=80μm. Note that similarly to the co-flow regime the results follow the same line with no temperature correlation. It proves that Eq. (11) remains valid for the opposing as for the co-flow configurations. In the same figure is also plotted the resulting (correlated) function obtained from the co-flow regime. The two behaviors differ in the low range, $Re_f<0.1$, but coincide for $Re_f>0.1$. This is due to a re-circulation phenomenon that does not pertain in the co-flow case. As forced convection increases the reversed flow diminishes and ϕ reduces to that obtained for the co-flow.

The transition from free convection dominated regime to mixed convection behavior as in the co-flow case occurs in a very narrow band of Re_f values as shown in Fig. 7, approximately $0.07<Re_f<0.1$. For values of Re_f smaller than 0.07 the drag force can be calculated from the expression for F_{fc}. For $Re_f>0.1$ the drag can be calculated from the co-flow results.

As noted the symmetry of the co-flow and the opposed flow patterns breaks down at low values of Re; this behavior deserves explanation. In the co-flow regime the direction of flow is always opposite to the direction of gravity, thus, no separation takes place and the behavior of the drag force is monotone with Re. In the opposed-flow regime, for sufficiently weak external flow a re-circulation zone emerges beneath the particle where the flow is reversed because of buoyancy forces. This re-circulation zone continues to grow as the external flow weakens and eventually will cover the whole sphere; this is exactly the point of rapid transition from positive to negative drag force depicted in Fig. 7. From now on the flow near the particle resembles free convection in a closed cavity (the walls of which are moving with the external velocity) and the drag force is almost unaffected by subsequent decrease of the external flow; in this region the flow field near the particle can be viewed as pure

free convection. Figure 8 visualizes growth of the buoyancy driven re-circulation around the particle for different Re_f obtained from the computational data.

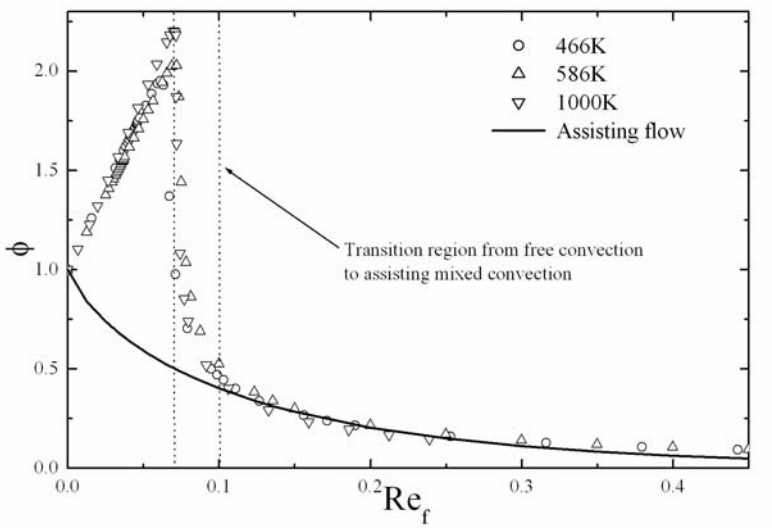

Fig. 7: Results for the function ϕ vs. Re_f are presented for 80μm particle at temperatures 466, 586, 1000 K (scattered points) and the curve for the co-flow case (solid line), with ambient temperature of 298 K.

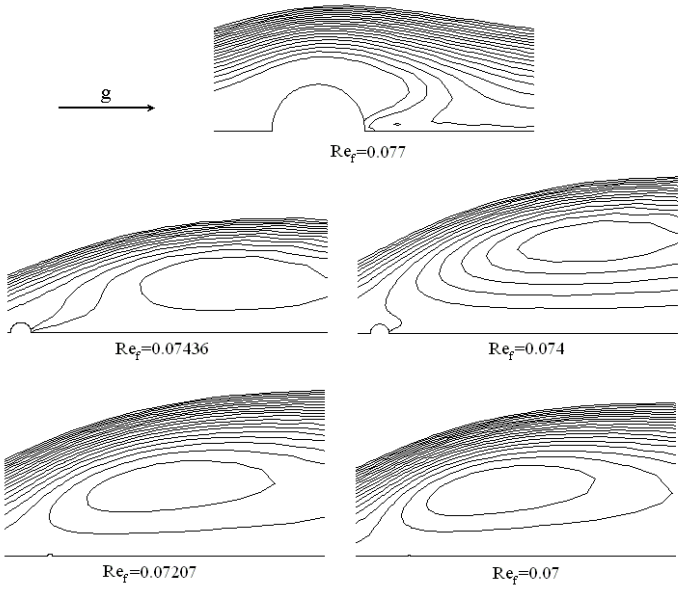

Fig. 8: A series of flow patterns by streamline contours of the mixed convection at various values of Re_f, showing re-circulation growth around the particle as Re_f decreases. The results were obtained for an 80 μm particle at 600 K, with ambient temperature of 298 K.

Acknowledgments

This study was partially supported by Binational Science Foundation (BSF) grant number 2000-163.

References

[1] Ya. B. Zel'dovich Zhur. 1937 Exp. Theor. Fiz **7** 1463 (in Russian)

[2] L. D. Landau, and E. M. Lifshitz 1999 Fluid Mechanics (Butterworth-Heinemann, Oxford) chapter V

[3] L. N. Gutman Prik. 1949 Mat. Mekh **13** 435 (in Russian)

[4] T. Fujii Int. 1963 J. Heat Mass Transfer **6** 597

[5] C. A. Hieber and B. Gebhart 1969 J. Fluid Mech **38** 137

[6] A. Acrivos, T. E. taylor 1962 Phys. Fluids **5** 387-394

[7] H. Brenner 1963 Chem. Eng. Sci **18** 109-115

[8] S. C. R. Dennis, J. D. A. Walker and J. D. Hudson 1973 J. Fluid Mech **60** 273-283

[9] T. S. Chen and A. Mucoglu 1977 Int. J. Heat Mass Transfer **20** 867-875

[10] A. Mucoglu and T. S. Chen 1978 J. Heat Transfer **100** 542-544

[11] K. L. Wong, S. C. Lee and C. K. Chen 1986 J. Heat Transfer **108** 860-865

[12] M. R. Cameron, D. R. Jeng and K. J. De Witt 1991 Int. J. Heat Mass Transfer **34** 582-587

[13] D. Katoshevski, B. Zhao, G. Ziskind and E. Bar-Ziv 2000 Aerosol Science **32** 73-86

[14] G. Ziskind, B. Zhao, D. Katoshevski, and E. Bar-Ziv 2001 Int. J. Heat Mass Transfer **44** 4381-4389

[15] E. Mograbi, G. Ziskind, D. Katoshevski, and E. Bar-Ziv 2002 Int. J. Heat Mass Transfer **45** 2423-2430

[16] E. Bar-Ziv, B. Zhao, E. Mograbi, D. Katoshevski, and G. Ziskind 2002 Phys. Fluids **14** 2015

[17] S. C. R. Dennis and J. D. A. Walker 1971 J. Fluid Mech **48**(4) 771-789

[18] V. I. Naidenov 1974 J. App. Math. Mech **38** 144

[19] E. Bar-Ziv and F. A. Sarofim 1990 Progress in Energy Combust. Sci **17** 1-65